Electronic Supporting Information

Zn-doped Fe_2TiO_5 Pseudobrookite-based Photoanodes Grown by Aerosol-Assisted Chemical Vapor Deposition

Miriam Regue,[†,‡,#] Ibbi Y. Ahmet,[§] Prince Saurabh Bassi,[§*] Andrew L. Johnson,[‖] Sebastian Fiechter,[§] Roel van de Krol,[§] Fatwa F. Abdi,[§] and Salvador Eslava[#*]

[†]Centre for Sustainable Chemical Technologies. Claverton Down, Bath, BA2 7AY, United Kingdom.

[‡]Department of Chemical Engineering, University of Bath, Claverton Down, Bath, BA2 7AY, United Kingdom

[§]Helmholtz-Zentrum Berlin für Materialien und Energie GmbH, Institute for Solar Fuels, Hahn-Meitner-Platz 1, Berlin 14109, Germany.

[‖]Department of Chemistry, University of Bath, Claverton Down, Bath, BA2 7AY, United Kingdom

[#]Department of Chemical Engineering, Imperial College London, London, SW7 2AZ, United Kingdom.

Corresponding Author

* E-mail: s.eslava@imperial.ac.uk

* E-mail: prince.bassi@helmholtz-berlin.de

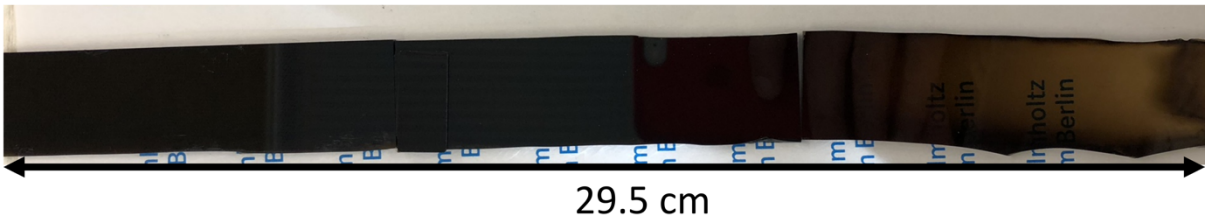

Figure S1. Representative photograph of as-deposited film on FTO-coated glass (Fe-Ti-O film prepared at 450 °C for 1 h by AA-CVD).

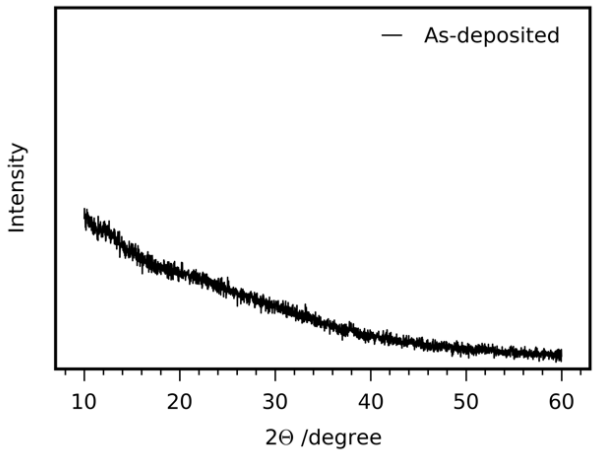

Figure S2. XRD pattern of as-deposited Fe-Ti-O at 450°C for 1h.

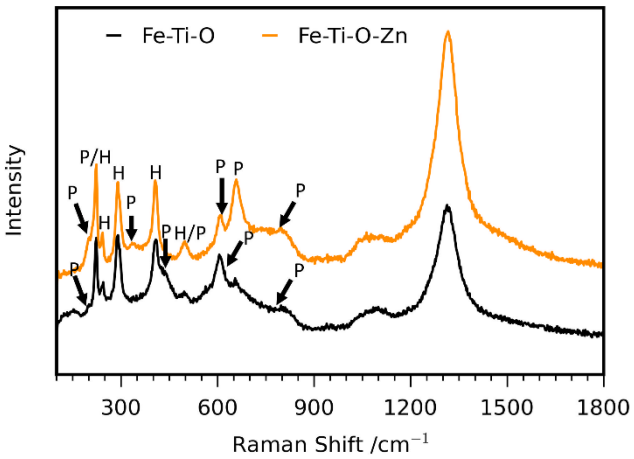

Figure S3. Raman spectra of Fe-Ti-O-Zn and Fe-Ti-O. P: Fe_2TiO_5 (pseudobrookite) and H: Fe_2O_3 (hematite).

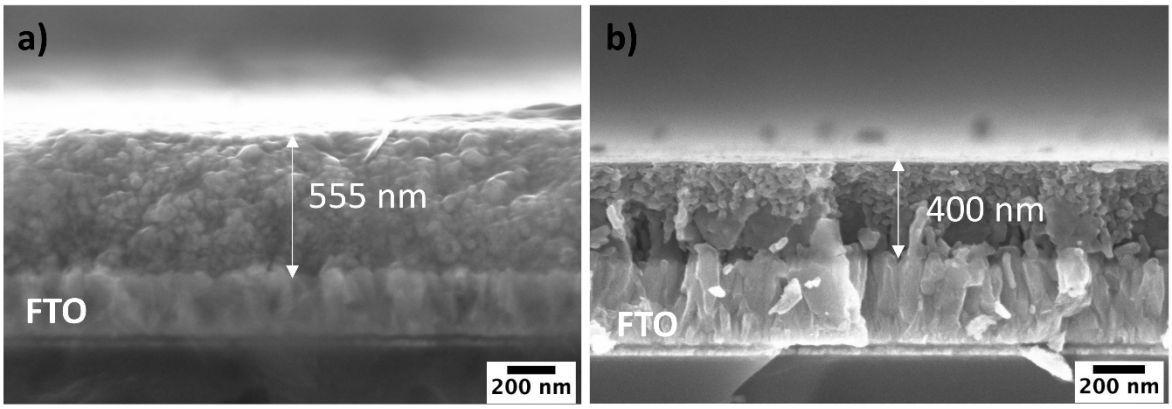

Figure S4. SEM cross-sectional micrographs of (a) Fe-Ti-O and (b) Fe-Ti-O-Zn.

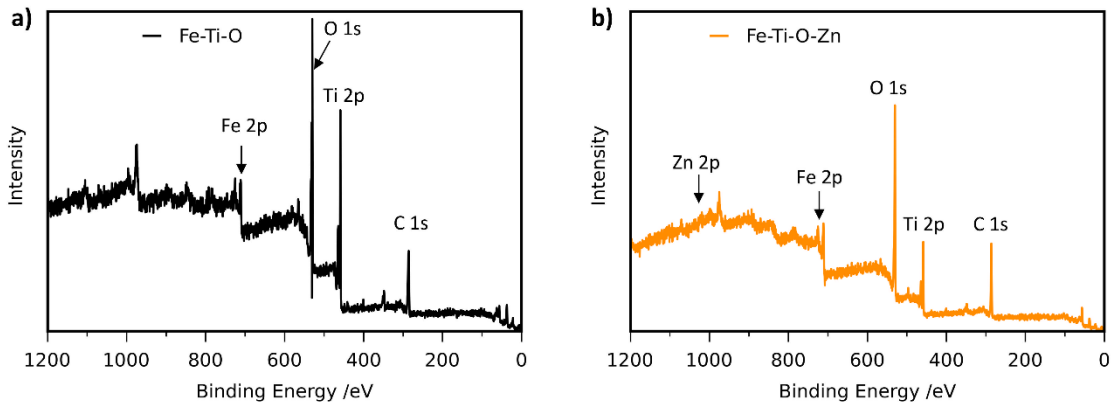

Figure S5. Survey XPS spectra of (a) Fe-Ti-O and (b) Fe-Ti-O-Zn thin film samples.

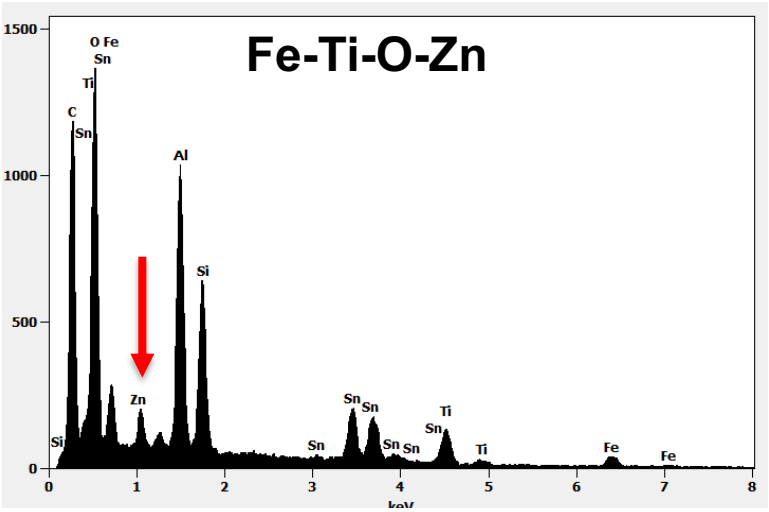

Figure S6. SEM-EDX spectrum of Fe-Ti-O-Zn sample measured with an acceleration voltage of 15 kV.

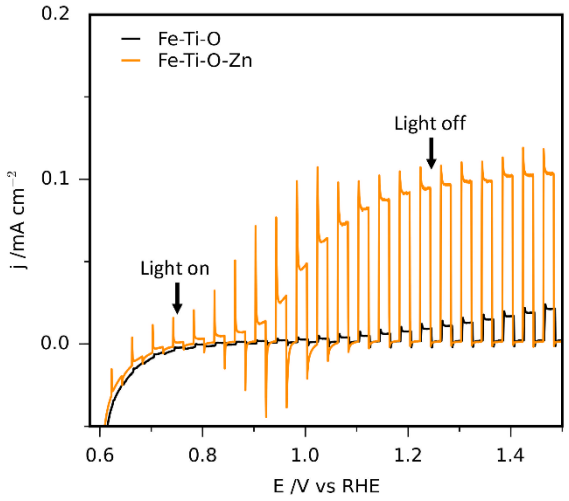

Figure S7. Front-side illumination j-V curves of Fe-Ti-O-Zn and Fe-Ti-O. All measurements were performed under chopped simulated sunlight (1 sun, AM 1.5) and in 1 mol L^{-1} NaOH (pH=13.6)

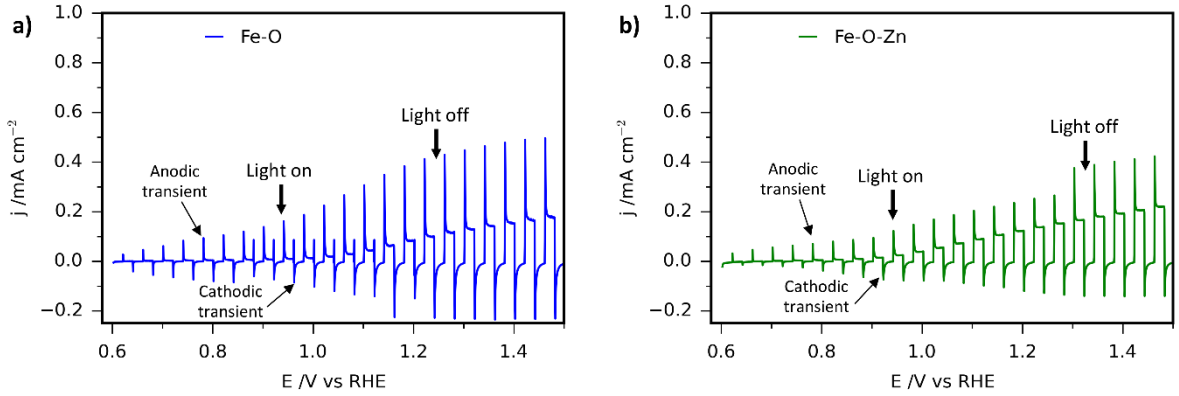

Figure S8. Back-side illumination *j-V* curves of Fe-O and Fe-O-Zn. All measurements were performed under chopped simulated sunlight (1 sun, AM 1.5) and in 1 mol L^{-1} NaOH (pH=13.6)

Table S1. Reported preparation methods, photocurrent performances and IPCE of Fe_2TiO_5-based photoanodes.

Composition	Preparation method[a]	Photocurrent density (mA cm^{-2})[b]	IPCE (%)[c]	Reference
Zn-doped Fe_2TiO_5 (major) & α-Fe_2O_3	AACVD	0.6	20	This work
Fe_2TiO_5 with Fe_2O_3 traces	Sol-gel synthesis and dip coating	0.05	Not reported	1
Fe_2TiO_5	Pulsed laser deposition	0.16	5	2
Fe_2TiO_5 with Ni_2FeO_x	Electrochemical	0.3	Not reported	3
Fe_2TiO_5 with SnO_x coating	solvothermal	0.36	10	4
Al^{3+}-surface-treated Fe_2TiO_5 with FeOOH as electrocatalyst	Electrospray + surface treatment	0.52	Not reported	5
F-surface modified Fe_2TiO_5	Electrospray + surface treatment	0.4	20	6
Fe_2TiO_5 inverse opal structure (IOS) with Ga_2O_3 underlayer and $(Ni_2CoFe)OOH$ electrocatalyst	Layer-by-layer self-assembly and hybrid microwave annealing	2.08	23	7
Fe_2TiO_5 nanotube arrays with TiO_2 underlayer, H_2 treatment and $FeNiO_x$ electrocatalyst	Hybrid microwave annealing (Use of anodized aluminum oxide as template)	0.93	Not reported	8

[a] Refers to the experimental method used for the growth of Fe_2TiO_5-based films. The methods used for electrocatalyst loadings or other treatments are omitted.

[b] Reported photocurrent density value at 1.23 V_{RHE} under simulated sunlight (AM 1.5G filter, 100 mW cm^{-2})

[c] IPCE at 350 nm measured at 1.23 V_{RHE}

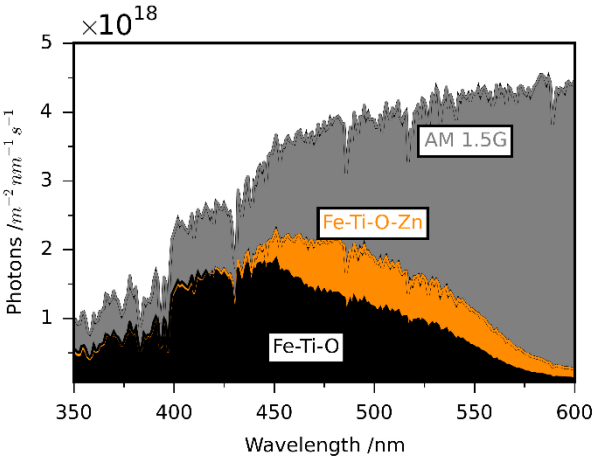

Figure S9. Number of photons absorbed from the solar visible light spectrum (AM 1.5G, 1 sun irradiance) for Fe-Ti-O-Zn and Fe-Ti-O.

Table S2. Theoretical maximum photocurrent density obtained by integrating the absorbance spectra with the AM 1.5G 1 sun irradiance spectrum.

Sample	j_{abs} (mA cm^{-2})
Fe-Ti-O	3.94
Fe-Ti-O-Zn	5.27

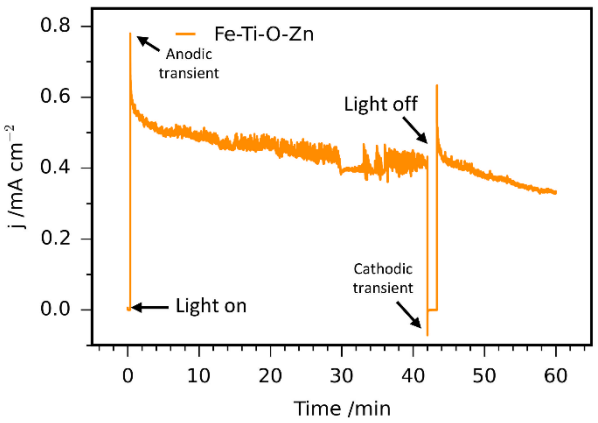

Figure S10. Photocurrent-time curve of Fe-Ti-O-Zn for 60 min under simulated sunlight (1 sun, AM 1.5) measured at 1. 23 V_{RHE} in 1 mol L^{-1} NaOH

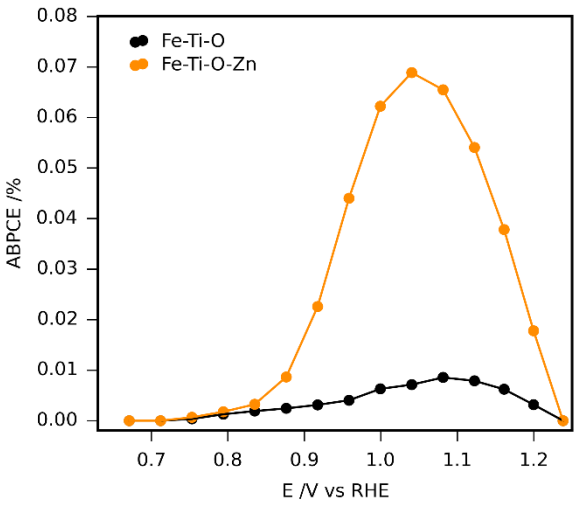

Figure S11. ABPCE curves of Fe-Ti-O and Fe-Ti-O-Zn.

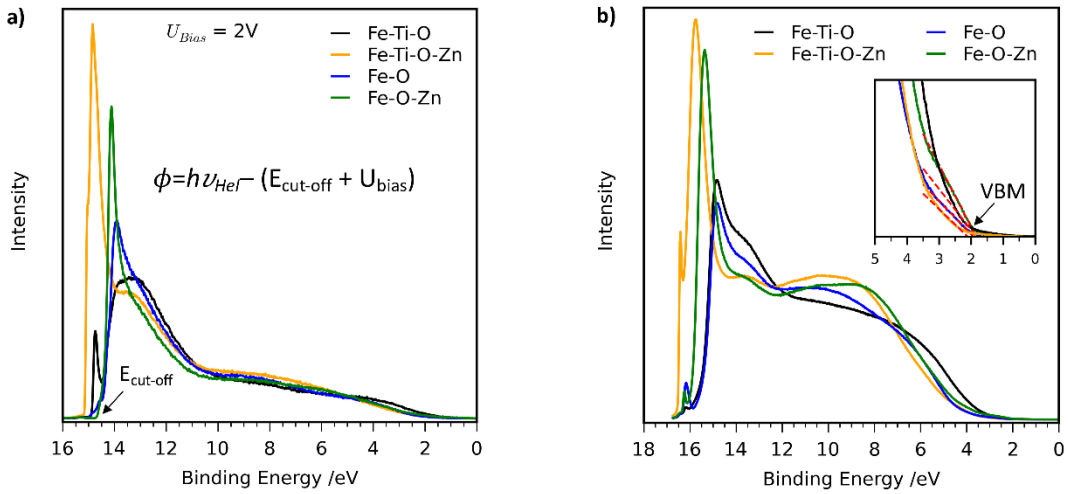

Figure S12. UPS measurements using an He I photon source (E=21.2 eV) with (a) an applied bias of 2 V and (b) without applied bias. From these measurements, $E_{cut\text{-}off}$, work function (ϕ) and valence band maximum (VBM) were determined.

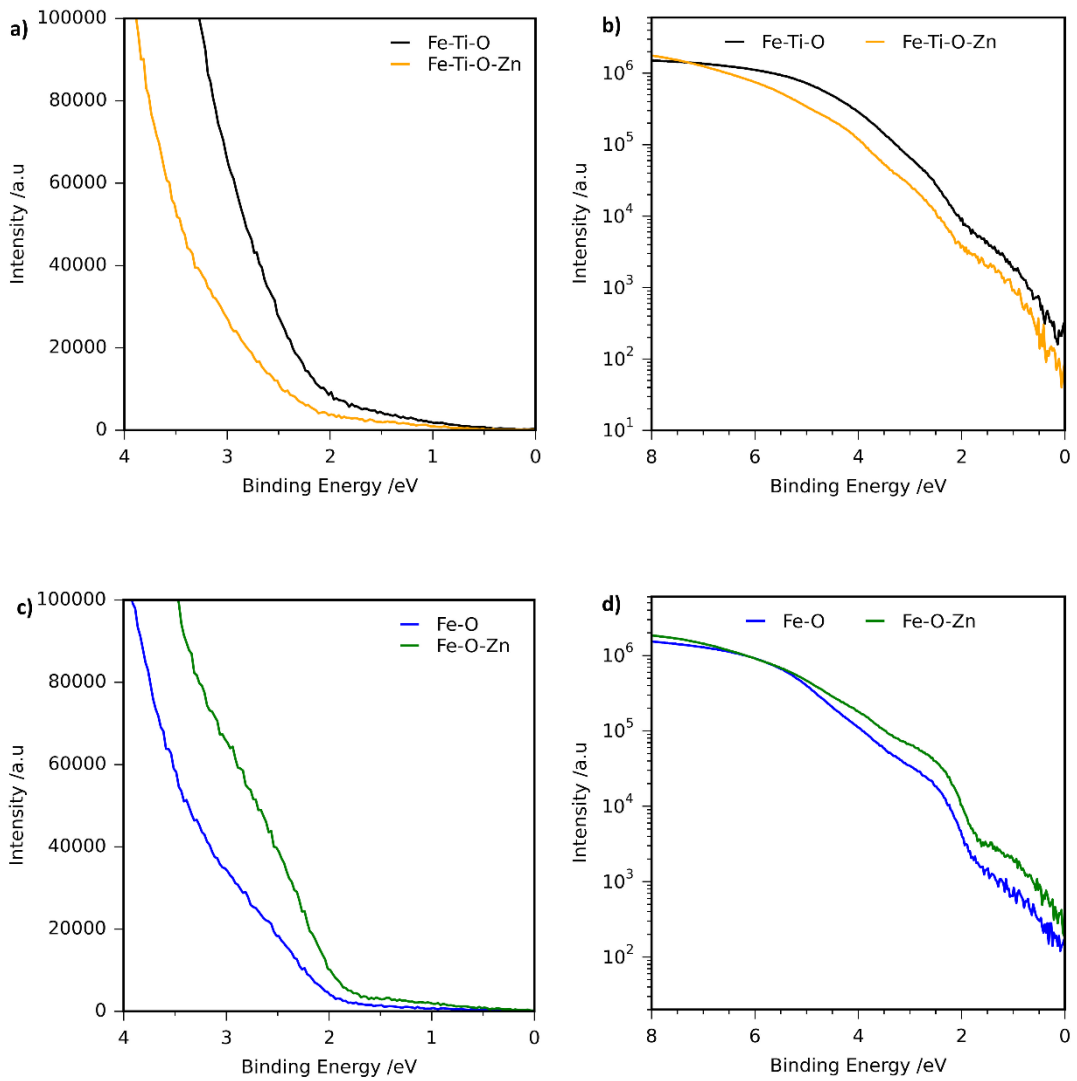

Figure S13. Zoomed-in UPS spectra using an He I photon source (E=21.2 eV) without applied bias plotted on a linear (a,c) and logarithmic scale (b,d). (a-b) Fe-Ti-O and Fe-Ti-O-Zn films. (c-d) Fe-O and Fe-O-Zn.

Table S3 Work function (ϕ) and valence band maximum (VBM)) values obtained from UPS measurements

Sample	Φ (eV)	VBM (eV)
Fe-Ti-O	4.36	1.83
Fe-Ti-O-Zn	4.07	2.10
Fe-O	4.77	1.93
Fe-O-Zn	4.88	1.82

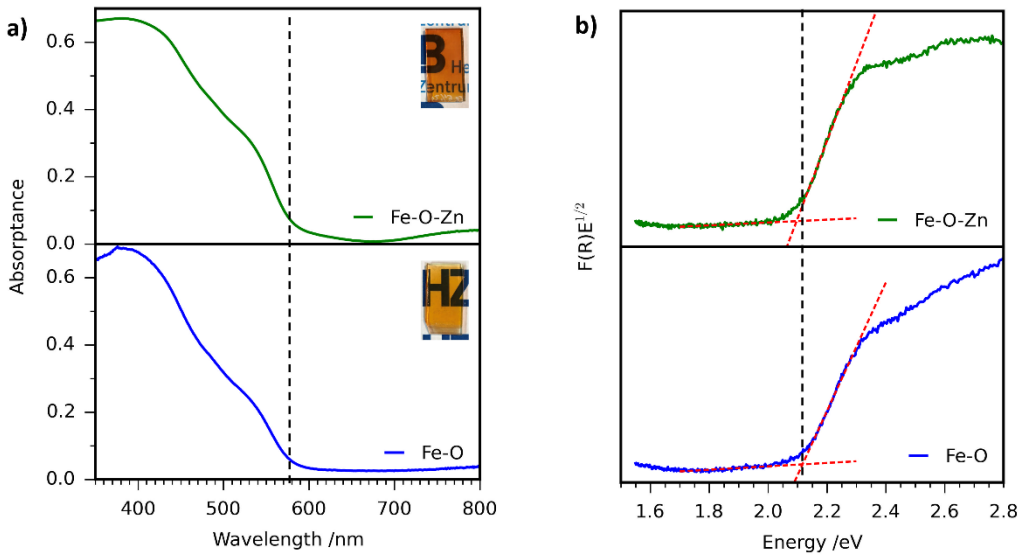

Figure S14. UV-*Vis absorptance* spectra and (b) Tauc plots measured via diffuse reflectance UV-Vis spectroscopy of Fe-O-Zn and Fe-O. Insets in (a) show photographs of all films prepared. Dashed vertical line indicates onsets for Fe-O samples. The logo is copyrighted by the Helmholtz-Zentrum Berlin für Materialien und Energie GmbH.

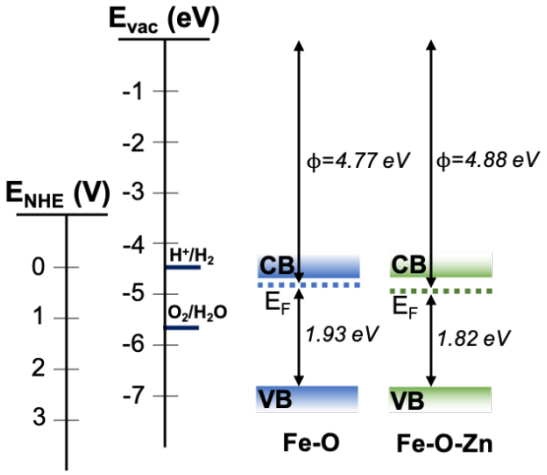

Figure S15. Schematic diagram of band level positions for Fe-O films calculated from UPS measurements (Figure S14†) with respect to the vacuum level and the normal hydrogen electrode (NHE) potential

References

(1) Courtin, E.; Baldinozzi, G.; Sougrati, M. T.; Stievano, L.; Sanchez, C.; Laberty-Robert, C. New Fe2TiO5-Based Nanoheterostructured Mesoporous Photoanodes with Improved Visible Light Photoresponses. *J. Mater. Chem. A* **2014**, *2* (18), 6567–6577. https://doi.org/10.1039/c4ta00102h.

(2) Bassi, P. S.; Xi, F.; Kölbach, M.; Gunder, R.; Ahmet, I. Y.; Krol, R. Van De; Fiechter, S. Pulsed Laser Deposited FeTiO Photoanodes for Photoelectrochemical Water Oxidation. *J. Phys. Chem. C* **2020**, *Just accep*. https://doi.org/10.1021/acs.jpcc.0c04396.

(3) Lee, D.; Baltazar, V. U.; Smart, T. J.; Ping, Y.; Choi, K. S. Electrochemical Oxidation of Metal-Catechol Complexes

as a New Synthesis Route to the High-Quality Ternary Photoelectrodes: A Case Study of Fe2TiO5 Photoanodes. *ACS Appl. Mater. Interfaces* **2020**, *12*, 29275–29284. https://doi.org/10.1021/acsami.0c05359.

(4) Bassi, P. S.; Chiam, S. Y.; Barber, J.; Wong, L. H. Hydrothermal Grown Nanoporous Iron Based Titanate, Fe 2 TiO 5 for Light Driven Water Splitting. *ACS Appl. Mater. Interfaces* **2014**, *24*, 2249–22495. https://doi.org/dx.doi.org/10.1021/am5065574.

(5) Kuang, S.; Wang, M.; Geng, Z.; Wu, X.; Sun, Y.; Ma, W.; Chen, D.; Liu, J.; Feng, S.; Huang, K. Enhancement of Fe 2 TiO 5 Photoanode through Surface Al 3+ Treatment and FeOOH Modification . *ACS Sustain. Chem. Eng.* **2019**, *7* (17), 14347–14352. https://doi.org/10.1021/acssuschemeng.9b03425.

(6) Wang, M.; Wu, X.; Huang, K.; Sun, Y.; Zhang, Y.; Zhang, H.; He, J.; Chen, H.; Ding, J.; Feng, S. Enhanced Solar Water-Splitting Activity of Novel Nanostructured Fe2TiO5 Photoanode by Electro- Spray and Surface F-Modificatio. *Nanoscale* **2018**, *10*, 6678–6683. https://doi.org/10.1039/C8NR01331D.

(7) Zhang, H.; Park, S. O.; Joo, S. H.; Kim, J. H.; Kwak, S. K.; Lee, J. S. Precisely-Controlled, a Few Layers of Iron Titanate Inverse Opal Structure for Enhanced Photoelectrochemical Water Splitting. *Nano Energy* **2019**, *62* (January), 20–29. https://doi.org/10.1016/j.nanoen.2019.05.025.

(8) Zhang, H.; Kim, J. H.; Kim, J. H.; Lee, J. S. Engineering Highly Ordered Iron Titanate Nanotube Array Photoanodes for Enhanced Solar Water Splitting Activity. *Adv. Funct. Mater.* **2017**, *27* (35), 1–9. https://doi.org/10.1002/adfm.201702428.